Received: 25 May 2024 | Revised: 15 September 2024 | Accepted: 19 September 2024

DOI: 10.1002/zamm.202400525

ORIGINAL PAPER

Nonlinear vibration and parametric excitation of magneto-thermo elastic embedded nanobeam using homotopy perturbation technique

Rajendran Selvamani[1] | **Prabhakaran Thangamuni**[1] | **Murat Yaylacı**[2,3,4] | **Mehmet Emin Özdemir**[5] | **Ecren Uzun Yaylacı**[6]

[1]Department of Mathematics, Karunya Institute of Technology and Sciences, Karunya Nagar, India

[2]Department of Civil Engineering, Recep Tayyip Erdogan University, Rize, Turkey

[3]Turgut Kıran Maritime Faculty, Recep Tayyip Erdogan University, Rize, Turkey

[4]Murat Yaylacı Luzeri R&D Engineering Company, Rize, Turkey

[5]Department of Civil Engineering, Cankiri Karatekin University, Çankırı, Turkey

[6]Faculty of Engineering and Architecture, Recep Tayyip Erdogan University, Rize, Turkey

Correspondence
Murat Yaylacı, Department of Civil Engineering, Recep Tayyip Erdogan University, Rize 53100, Turkey.
Email: murat.yaylaci@erdogan.edu.tr

The present study focuses on the modeling and analyzing the nonlinear vibration patterns and parametric excitation of embedded Euler–Bernoulli nanobeams subjected to thermo-magneto-mechanical loads. The Euler–Bernoulli nanobeam is developed with external parametric excitation. The governing equation of motion is derived by utilizing nonlocal continuum theory and nonlinear von Karman beam theory. Subsequently, the homotopy perturbation technique is employed to determine the vibration frequencies. Finally, the modulation equation of Euler–Bernoulli nanobeams is derived for simply supported boundary condition. In order to validate our findings, we conduct a comparative analysis against existing literature, thereby underscoring the effectiveness and robustness of our proposed methodology. The influence of stress, magnetic potential, temperature, damping coefficient, Winkler coefficient, and nonlocal parameters are tested numerically on nonlinear frequency-amplitude and parametric excitation–amplitude responses. The numerical examples indicate the significant impact of physical variables on the nonlinear frequency and parametric excitation. The primary objective of this study is to investigate the effects of external physical variables on the dynamic behavior of nanobeams, particularly in nonlinear regimes. This study provides insights into the design and control of nanostructures under complex load conditions, contributing to developing advanced materials and nanosystems.

1 | INTRODUCTION

The captivating electromechanical properties of carbon nanostructures, such as carbon nanotubes and nanobeams, have drawn the interest of numerous researchers and scholars in the fields of advanced materials and the design process in engineering. These nanostructures have found application in a variety of electromechanical devices, including translucency of light [1–3], vibratory systems [4–7], gas atom diagnosis [8], storage units [9], and amalgamated substances [10]. Nevertheless, even though the importance of small-scale effects on the characteristics and properties of nanostructures

is recognized, more than classical plate theory (CLPT) is needed in assessing the size effect in these structures [11]. As a result, the nonlocal elasticity theory, introduced by Eringen [12], has been widely adopted to examine the size effect of nanostructures. Alongside implementing nonlocal elasticity theory, researchers have conducted numerous theoretical investigations [13–24] and made significant advancements. Presently, the majority of research on micro/nano beams has been directed towards their nonlinear properties. Notably, the nonlinear or high-amplitude vibration of beams, whether nano or micro, subjected to significant displacements, holds a crucial position in engineering literature and investigations. Several notable works have contributed to this field: Simsek [25, 26] explored the nonlinear vibration of nanobeams using nonlocal elasticity and strain gradient theories, revealing the impact of small-scale effects regarding the nonlinear frequency response. Nazemnezhad and Hosseini-Hashemi [27] examined the nonlinear vibration behavior of functionally graded (FG) nanobeams under different boundary conditions, emphasizing the influence of the gradient index on nonlinear vibration characteristics. Additionally, Nourbakhsh et al. [28] utilized von Karman theory to analyze the effect of nonlinearity on the nonlinear frequency response of microbeams. Oskouie et al. [29] presented the nonlinear frequency response of viscoelastic Euler–Bernoulli nanobeams, emphasizing the impact of viscoelastic properties on nonlinear vibration characteristics. Meanwhile, Ghadiri et al. [30] utilized the multiple time scales method to study the nonlinear forced vibration of nanobeams experiencing a moving concentrated load supported by a viscoelastic foundation. He [31] investigated a coupling method utilizing both homotopy perturbation techniques (HPT) for analyzing nonlinear problems. Additionally, He [32] provided a new interpretation of the HPT in an addendum. Eltaher et al. [33] examined the coupling effects of nonlocal and surface energy on the vibration analysis of nanobeams. Reddy [34] discussed nonlocal theories about beams' bending, buckling, and vibration. Aydogdu [35] investigated a comprehensive nonlocal beam theory and its application to analyze nanobeams' bending, buckling, and vibration. More recently, recognizing the importance of parametric excitation in electromechanical systems, researchers have investigated its impact on energy harvesting systems [36–38], using a Duffing oscillator to simulate the performance of energy harvesters. Additionally, researchers utilized parametric excitation to study tapered-composite plates' nonlinear vibration [39]. Moreover, Wang [40] analyzed the effect of van der Waals interaction on the instability of double-walled nanobeams subjected to parametric excitation. Similarly, Krylov et al. [41] discussed the pull-in instability of micro devices under parametric excitation, employing Mathieu and Hill's equations. Yan et al. [42] offered valuable insights into the behavior of Timoshenko beams subjected to parametric and external excitations. Meanwhile, Eringen [43, 44] examined the theory of nonlocal polar elastic continua, investigating the differential equations governing nonlocal elasticity and exploring solutions related to screw dislocation and surface waves. Reddy [45, 46] contributed to the field by investigating continuum mechanics and delving into nonlocal nonlinear formulations for the bending of beams and plates, encompassing both classical and shear deformation theories. Emam [47] examined the static and dynamic analysis of post-buckling in geometrically imperfect composite beams, whereas Emam and Nayfeh [48] concentrated on the post-buckling behavior and free vibrations of composite beams. Murmu et al. [49] investigated the influence of in-plane magnetic fields on the transverse vibration of single-layer graphene sheets embedded within a material, employing an equivalent nonlocal elasticity approach. Kitipornchai et al. [50] presented a continuum model for analyzing the vibration characteristics of multilayered graphene sheets. Nayfeh and Mook [51] studied nonlinear oscillations, while Nazemnezhad and Hosseini-Hashemi [27] concentrated on nonlocal nonlinear free vibration of FG nanobeams. Nazemnezhad et al. [52, 53] introduced a semi-analytical method to address the nonlinear dynamic response of S–S and C–C beams under large vibration amplitudes, encompassing a comprehensive theory and applying a single-mode approach to analyze free and forced vibration and further expanded their study to include a multimode approach to steady-state forced periodic response. Azrar et al. [54, 55] examine the dynamic stability and vibrations of a bogie system on a flexible track and the stability of parametric vibrations in a cross-ply laminated composite plate. Characteristics and behaviors of various nanobeam configurations under different environmental and boundary conditions were investigated by refs. [56–64]. A literature review suggests that the nonlinear vibration and parametric excitation of magneto-thermo-elastic embedded nanobeams have yet to be extensively explored. This research thoroughly investigates these aspects by examining the nonlinear vibration behaviors and parametric excitation effects on Euler–Bernoulli nanobeams embedded in a medium, under thermo-magneto-mechanical loads and external parametric excitation. Initially, a simplified model of the nanobeam is developed, followed by the application of an external axial force to induce parametric excitation. The study then derives the governing nonlinear differential equation of motion using nonlocal continuum theory and nonlinear von Karman beam theory, which is solved using the HPT. The modulation equation and dynamic instability of the Euler–Bernoulli nanobeam are derived, allowing for an analysis of both trivial and nontrivial steady-state solutions. Finally, the plots are given with physical explanations for stress, magnetic potential, temperature, damping coefficient, Winkler coefficient, and nonlocal parameters on nonlinear frequency-amplitude and parametric excitation–amplitude responses.

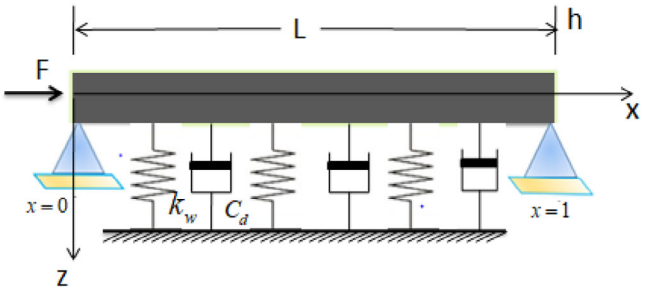

FIGURE 1 Geometry of the problem.

2 | FORMULATING THE PROBLEM

Figure 1 illustrates the schematic of a nanobeam embedded in a visco-Pasternak foundation, subjected to an axial force (F) along the x-axis with a height h and length L. The axial force is represented as a function undergoing harmonic excitation with frequency ($\bar{\Omega}$). Moreover, the vertical displacement of the nanobeam is indicated by w along the z-axis.

2.1 | Constitutive relations

By Eringen's nonlocal elasticity theory [11, 12, 43, 44], the stress experienced at a reference point X is postulated to be contingent upon the strain field throughout the body at each point X'. The nonlocal stress tensor σ at point X is formulated as follows:

$$\sigma = \int_V K\left(\left|X' - X\right|, \tau\right) \sigma'(X')dX' \tag{1}$$

Here, σ' denotes the classical stress tensor and $K(|X' - X|)$ represents the Kernel function, which signifies the nonlocal modulus. Eringen [12, 44] illustrates that it is feasible to express the integral constitutive relation in an equivalent differential form as:

$$\left(1 - (e_0 a)^2 \nabla^2\right) \sigma = \sigma' \tag{2}$$

$\nabla^2 = \frac{\partial^2}{\partial x^2} + \frac{\partial^2}{\partial y^2}$ represents the Laplacian operator, $(e_0 a)$ introduces the nonlocal parameter, e_0 is a material-specific constant, and a is the internal characteristic length. Determining the value of e_0 typically involves experimental methods or matching the dispersion relation of plane waves with those of atomic lattice dynamics. Subsequently, the nonlocal constitutive relation for the Euler–Bernoulli nanobeam can be expressed as:

$$\sigma_{xx} - (e_0 a)^2 \frac{\partial^2 \sigma_{xx}}{\partial x^2} = E\varepsilon_{xx} \tag{3}$$

Here, σ_{xx}, ε_{xx} denote the normal stress and strain, respectively, while E represents Young's modulus. Following the Euler-Bernoulli beam model, the axial force and the resultant bending moment can be formulated as

$$\{\mathrm{N}, \mathrm{M}\} = \int_A \sigma_x (1, z)\, dA \tag{4}$$

Here, z represents the transverse coordinate in the deflection direction, and A denotes the area of the cross-section of the nanobeam. Utilizing classical beam theory as outlined by Reddy [45, 46], the displacements can be expressed as follows:

$$u_1(x, z, t) = u(x, t) - z\frac{\partial w}{\partial x}, \quad u_2 = 0, \quad u_3(x, z, t) = w(x, t) \tag{5}$$

In Equation (5), u and w represent the axial and transverse displacements of the nanobeam along the x and z directions, respectively. Now, considering the nonlinear von Karman strain, we can express it as:

$$\varepsilon = \varepsilon_0 + zk \tag{6}$$

where ε is the strain vector, and ε_0 and k are the nonlinear strain vector and the change in the curvature vector, respectively, defined as follows:

$$\varepsilon_0 = \frac{\partial u_0}{\partial x} + \frac{1}{2}\left(\frac{\partial w}{\partial x}\right)^2, \; k = -\frac{\partial^2 w}{\partial x^2} \tag{7}$$

In this context, u_0 represents the initial axial displacement in the strain expression, which captures the axial deformation before accounting for the additional effects due to transverse displacements and curvature. From Equations (3)–(7), the axial load and the bending moment as follows:

$$\left(1-(e_0a)^2\nabla^2\right)N = EA\varepsilon_0 \left(1-(e_0a)^2\nabla^2\right)M = EIk \tag{8}$$

where, $I = \int_A z^2 dA$ represents the moment of inertia. Therefore, the equation of motion can be expressed as refs. [47, 48]:

$$EI\frac{\partial^4 w}{\partial x^4} - \frac{\partial}{\partial x}\left(N\frac{\partial w}{\partial x}\right) + (e_0a)^2\frac{\partial^3}{\partial x^3}\left(N\frac{\partial w}{\partial x}\right) + \rho A\frac{\partial^2}{\partial t^2}\left[w-(e_0a)^2\frac{\partial^2 w}{\partial x^2}\right] = f-(e_0a)^2\frac{\partial^2 f}{\partial x^2} \tag{9}$$

The axial normal force N can be determined as follows:

$$N = M_x + T_x + N_x + Fcos\Omega t - \left[\frac{EA}{2L}\right]\int_0^L \left(\frac{\partial w}{\partial x}\right)^2 dx \tag{10}$$

In Equation (10) M_x, T_x, N_x represents a uniaxial magnetic field, thermal load caused by temperature change and in-plane load caused by initial stress, respectively. Additionally, the term of $Fcos\Omega t$ is also the axial force capable of inducing parametric excitation, and we can define the parameters of the axial normal force as follows:

$$M_x = \eta H_x^2\frac{\partial^2 w}{\partial x^2}, \quad T_x = \alpha EAT, \quad N_x = \xi\sigma_0 \tag{11}$$

Here, H_x, η represents the in-plane uniaxial magnetic field and the magnetic field permeability, respectively. Specifically, M_x explains the Lorentz force along the x-axis [49]. Regarding T_x, α, A, and T denote the coefficient of thermal expansion, the cross-sectional area and the difference between the temperature and its initial reference temperature, respectively. Moreover, ξ and σ_0 are the compression ratio and the initial stress, respectively. In this study, it is assumed that $\xi = 1$ and initial stress is along the x-axis direction. Additionally, in Equation (9), f is defined as follows:

$$f = K_w w + c_d\frac{\partial w}{\partial t} \tag{12}$$

where, k_w and c_d represent the linear coefficient of Winkler and damper modulus parameter, respectively. The Winkler type foundation can be characterized based on the model from reference [50]. Finally, to obtain the equation of motion, we substitute Equations (10)–(12) into Equation (9) as follows:

$$\begin{aligned} &-EI\frac{\partial^4 w}{\partial x^4} - \left\{M_x + T_x + N_x + Fcos\Omega t - \left[\frac{EA}{2L}\right]\int_0^L \left(\frac{\partial w}{\partial x}\right)^2 dx\right\}\frac{\partial^2 w}{\partial x^2} + c_d\frac{\partial w}{\partial t} + K_w w \\ &+ (e_0a)^2\frac{\partial^4 w}{\partial x^4}\left\{M_x + T_x + N_x + Fcos\Omega t - \left[\frac{EA}{2L}\right]\int_0^L \left(\frac{\partial w}{\partial x}\right)^2 dx\right\} \\ &- (e_0a)^2 K_w\frac{\partial^2 w}{\partial x^2} - (e_0a)^2 c_d\frac{\partial^3 w}{\partial t\partial x^2} = \rho A\left[\frac{\partial^2 w}{\partial t^2} - (e_0a)^2\frac{\partial^4 w}{\partial t^2\partial x^2}\right] \end{aligned} \tag{13}$$

To facilitate a good comparison between results, nondimensional parameters can be articulated as follows:

$$X = \frac{x}{L}, \ w_0 = \frac{W}{L}, \gamma = \frac{e_0 a}{L}, \ K_w = \frac{K_w L^4}{EI}, \ T_x = \frac{T_x L^2}{EI}, N_x = \frac{N_x L^2}{EI}, M_x = \frac{M_x L^2}{EI}, \ c_d = c_d \sqrt{\frac{L^4}{EI}}, \ \Omega = \Omega \sqrt{\frac{\rho A L^4}{EI}} \tag{14}$$

By incorporating these nondimensional parameters and substituting them into Equation (13), the governing equation of nanobeam can be derived as follows:

$$\begin{aligned} &\frac{\partial^4 w_0}{\partial X^4} - \left\{ M_x + T_x + N_x + F cos\Omega t - \left[\frac{EA}{2L}\right] \int_0^L \left(\frac{\partial w_0}{\partial x}\right)^2 dx^{\%} \right\} \frac{\partial^2 w_0}{\partial X^2} + c_d \frac{\partial w_0}{\partial t} + K_w w_0 \\ &+ (\gamma)^2 \frac{\partial^4 w_0}{\partial X^4} \left\{ M_x + T_x + N_x + F cos\Omega t - \left[\frac{EA}{2L}\right] \int_0^L \left(\frac{\partial w_0}{\partial x}\right)^2 dx^{\%} \right\} (\gamma)^2 K_w \frac{\partial^2 w_0}{\partial X^2} - \%(\gamma)^2 c_d \% \frac{\partial^3 w_0}{\partial t \partial X^2} \\ &= \left(\frac{\partial^2 w_0}{\partial t^2} - (\gamma)^2 \frac{\partial^4 w_0}{\partial t^2 \partial X^2} \right) \end{aligned} \tag{15}$$

3 | HPT

The HPT offers an analytical approximate solution for problems that exhibit continuity within the solution domain. This technique involves considering a differential equation.

$$Ly + Ny = f(x), \ x \epsilon \Omega \tag{16}$$

Under the boundary conditions, $B\left(y, \frac{\partial y}{\partial x}\right) = 0$, $x \in \Gamma$. Here, L is the linear operator, N is the nonlinear operator, B is the boundary operator, Γ represents the boundary of the domain Ω, and (x) is the known analytic function. HPT defines a Homotopy as $\upsilon(x, p) = \Omega \times [0,1] \to R$ that satisfies the following inequalities:

$$H(\upsilon, p) = (1-p)[L(\upsilon) - L(y_0)] + p[L(\upsilon) + N(\upsilon) - f(x)] = 0 \tag{17}$$

or

$$H(\upsilon, p) = L(\upsilon) - L(y_0) + pL(y_0) + p[N(\upsilon) - f(x)] = 0 \tag{18}$$

where $x \epsilon \Omega$ and $p \epsilon [0,1]$, and y_0 is an initial approximation which satisfies the boundary condition. Now from Equations (17) to (18) one can obtain:

$$\begin{aligned} H(\upsilon, 0) &= L(\upsilon) - L(y_0) = 0, \\ H(\upsilon, 1) &= L(\upsilon) + N(\upsilon) - f(x) = 0. \end{aligned} \tag{19}$$

In topology, $L(\upsilon) - L(y_0)$ and $L(\upsilon) + N(\upsilon) - f(x)$ is explore the homotopic.
Consider the power series solution of (17) and (18) as follows:

$$\upsilon = \upsilon_0 + p\upsilon_1 + p^2\upsilon_2 + p^3\upsilon_3 + \cdots \tag{20}$$

Hence, the approximate solution of (17) can be obtained:

$$y = \lim_{p \to 1} \upsilon = \upsilon + \upsilon_0 + \upsilon_1 + \upsilon_2 + \cdots \tag{21}$$

3.1 | Implementation of boundary conditions in HPT

3.1.1 | Simply supported-simply supported (S–S)

$$w_0 = \frac{d^2w_0}{dx^2} = \frac{d^4w_0}{dx^4} = 0 \quad \text{at } x = 0,$$
$$w_0 = \frac{d^2w_0}{dx^2} = \frac{d^4w_0}{dx^4} = 0 \quad \text{at } x = 1 \tag{22}$$

So, after using the above boundary conditions in the nth order approximate solution the system of homogenous equation can be written as,

$$M(\lambda)[A\ B\ C\ D]^T = 0 \tag{23}$$

For a nontrivial solution, the determinant of the coefficient matrix must be zero. The determinant of the coefficient matrix yields a characteristic equation in terms of λ. Positive real roots of this equation are the normalized free vibration frequencies for the case considered.

3.2 | HPT formulation for present problem

Consider the nondimensional differential Equation (15); this equation can be reformulated as:

$$\frac{\partial^4 w_0}{\partial X^4} = \frac{N}{\gamma^2 N - 1}\frac{\partial^2 w_0}{\partial X^2} + \frac{1}{\gamma^2 N - 1}\frac{\partial^2 w_0}{\partial t^2} - \frac{\gamma^2}{\gamma^2 N - 1}\frac{\partial^4 w_0}{\partial t^2 \partial X^2} - c_d\frac{\partial w_0}{\partial t} - K_w w_0 \tag{24}$$

The homotopy can be applied as ref. [59]:

$$\frac{\partial^4 w_0}{\partial X^4} = p\left[\frac{N}{\gamma^2 N - 1}\frac{\partial^2 w_0}{\partial X^2} + \frac{1}{\gamma^2 N - 1}\frac{\partial^2 w_0}{\partial t^2} - \frac{\gamma^2}{\gamma^2 N - 1}\frac{\partial^4 w_0}{\partial t^2 \partial X^2} - c_d\frac{\partial w_0}{\partial t} - K_w w_0\right] \tag{25}$$

where p is the homotopy parameter, $p \in [0, 1]$. It is obvious that when $p = 0$, the equation becomes homogenous that is,

$$\frac{\partial^4 w}{\partial X^4} = 0 \tag{26}$$

The initial approximation W_0 is obtained by solving the homogenous Equation (26), hence

$$w_0 = Ax^4 + Bx^3 + Cx^2 + D \tag{27}$$

The basic assumption of the HPT is that the solution of Equation (25) can be written as power series in p

$$w_{aprrox} = w_0 + pw_1 + p^2 w_2 + \cdots \tag{28}$$

By substituting the value of w_{aprrox} from Equation (28) in Equation (25)

$$\begin{aligned}\frac{\partial^4}{\partial X^4}\left[w_0 + pw_1 + p^2w_2 + \cdots\right] = p\Bigg[&\frac{N}{\gamma^2 N - 1}\frac{\partial^2}{\partial X^2}\left[w_0 + pw_1 + p^2w_2 + \cdots\right] + \frac{1}{\gamma^2 N - 1}\frac{\partial^2}{\partial t^2}\left[w_0 + pw_1 + p^2w_2 + \cdots\right] \\ &- \frac{\gamma^2}{\gamma^2 N - 1}\frac{\partial^4}{\partial t^2 \partial X^2}\left[w_0 + pw_1 + p^2w_2 + \cdots\right] - c_d\frac{\partial}{\partial t}\left[w_0 + pw_1 + p^2w_2 + \cdots\right] \\ &- k_w\left[w_0 + pw_1 + p^2w_2 + \cdots\right]\Bigg]\end{aligned} \tag{29}$$

TABLE 1 Comparison of amplitude ratio value with literature data.

Amplitude ratio	Ref. [27]	Ref. [52]	Present work
1	1.0937	1.0892	1.0758
2	1.3750	1.3178	1.3690
3	1.8438	1.6257	1.8401

Now comparing the coefficients of p in Equation (29) the recurrence relation can be obtained as

$$\frac{\partial^4 w_i}{\partial X^4} = \left[\frac{N}{\gamma^2 N-1}\frac{\partial^2 w_{i-1}}{\partial X^2} + \frac{1}{\gamma^2 N-1}\frac{\partial^2 w_{i-1}}{\partial t^2} - \frac{\gamma^2}{\gamma^2 N-1}\frac{\partial^4 w_{i-1}}{\partial t^2 \partial X^2} - c_d\frac{\partial w_{i-1}}{\partial t} - K_w w_{i-1}\right] \tag{30}$$

where $i \geq 1$ and initial guess w_0 is given in Equation (27).

The solution to Equation (24) can be approximated as per ref. [31].

$$w_0 = \lim_{p\to 1} w_{aprrox} = w_0 + w_1 + w_2 + \cdots \tag{31}$$

The convergence of the series in Equation (31) is proved in refs. [31, 32].

4 | NUMERICAL RESULTS

The frequency ratio (ω_{NL}, ω_L) at different maximum amplitude-to-radius (ω_{max}/r) ratios of isotropic beam with simply supported boundary conditions.

In this section, numerical results are examined based on applying both thermo-magneto-mechanical loading and external parametric excitation. The focus lies in understanding the impact of parametric excitation by examining instability regions and bifurcation points. Key parameters are defined across various regions of the graph to aid comprehension. This helps to elucidate the concepts and enhance clarity. The system's material properties, including those of the nanobeam and elastic matrix, consist of the following parameters: Young's modulus $E = 1100$ Gpa, mass density $\rho = 1.3$ g/cm^3, Winkler coefficient $k_w = 0.5$ and a viscoelastic damping coefficient of 3×10^{-7} Pa.s. Additionally, the nanobeam diameter is $d = 3$ nm, and the small-scale parameter is considered smaller than 2 nm, according to reference [34].

Firstly, Table 1 is presented to verify the formulation's accuracy. The numerical results of the present study reported in the table are compared with other available research and literature [27, 52] so that they are partly similar and close to our research. Table 1 shows the nonlinear frequency ratio (ω_{NL}, ω_L) for amplitude-to-radius (ω_{max}/r) ratio of isotropic beam with simply supported boundary conditions. The nonlinear frequency ratio is tabled for different amplitudes ratio [1, 2, 5]. Due to using a similar analytical approach, the results presented in ref. [27] show more accuracy than the present work's numerical results.

Figure 2 illustrates the frequency at which parametric excitation induces nonlinear behavior, representing the frequency at which the system exhibits nonlinear behavior, such as large amplitude vibrations. The relationship between this nonlinear frequency and the amplitude of the parametric excitation varies depending on the nondimensional damping coefficient c_d. Higher oscillation amplitudes are achievable when c_d is low, indicating less damping in the system. Consequently, the nonlinear frequency tends to be higher in such cases. This implies that the nonlinear frequency increases with a rise in the parametric excitation amplitude, producing a more intense nonlinear response. In summary, lower values of c_d cause the nonlinear frequency to decrease as the amplitude increases, whereas lower values of the nondimensional damping coefficient cause the nonlinear frequency to increase with increasing amplitude of parametric stimulation. Figure 3 displays the relationship between the force and nonlinear frequency amplitude concerning the nondimensional Winkler coefficient k_w. The graph illustrates that the force amplitude decreases as the Winkler coefficient increases. However, it is noteworthy that the Winkler coefficient does not influence the occurrence of bifurcation points. In other words, while changes in k_w affect the force amplitude, they do not impact the system's bifurcation behavior. Figure 4 shows how the nonlinear frequency varies with the magnitude of parametric excitation for a range of uniaxial magnetic field values. The force nonlinear frequency of a system subjected to a uniaxial magnetic field denotes the frequency at which the system's response turns nonlinear due to the magnetic field's effect. The system's response to the magnetic field may exhibit nonlinear behavior as

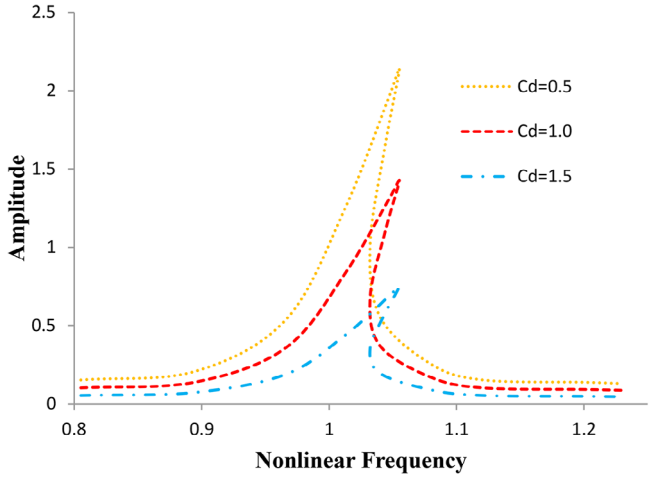

FIGURE 2 The effect of nonlinear frequency on the amplitude of parametric excitation for different values of damping coefficient (c_d).

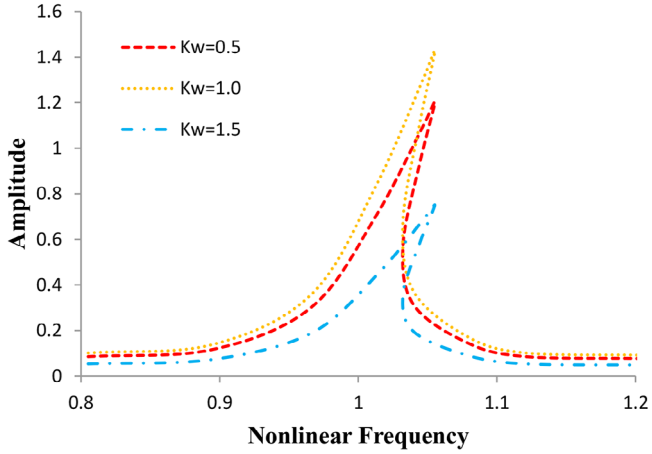

FIGURE 3 The effect of nonlinear frequency on the amplitude of parametric excitation for different values of Winkler coefficient (k_w).

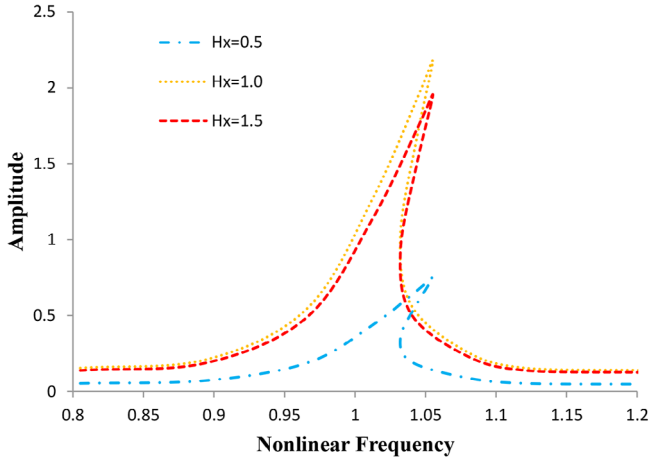

FIGURE 4 The effect of nonlinear frequency on the amplitude of parametric excitation for different values of uniaxial magnetic field (H_x).

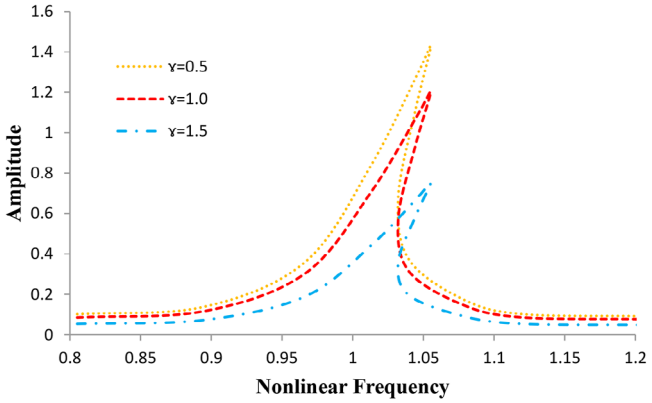

FIGURE 5 The effect of nonlinear frequency on the amplitude of parametric excitation for different values of nonlocal parameter (γ).

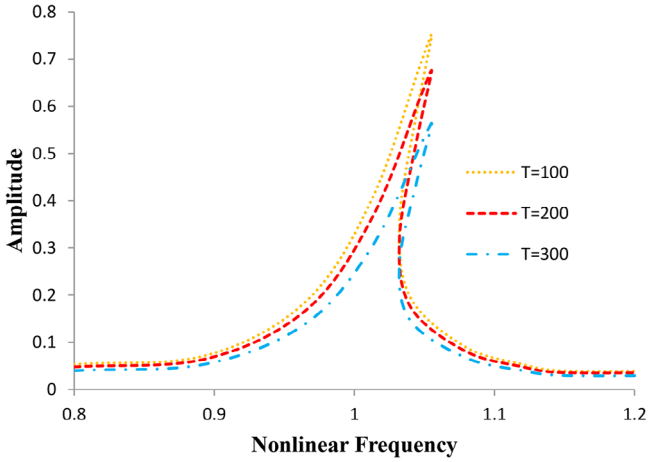

FIGURE 6 The effect of nonlinear frequency on the amplitude of parametric excitation for different values of temperature (T).

the amplitude of parametric stimulation increases, resulting in changes in the nonlinear frequency. Illustrated in Figure 5 is the nonlocal parameter's effect on the nonlinear frequency-response curves. It is clear from the graph that increasing the nonlocal parameter reduces the hardening behavior while enhancing the bending stiffness. The relationship between the parametric excitation amplitude and the force amplitude of the nonlinear frequency is shown for different temperatures in Figure 6. Additionally, it is observed that an increase in the temperature gradient results in a higher amplitude at the lower limit point bifurcation. Conversely, elevating the initial imperfection amplitude leads to greater response amplitude at the higher limit point bifurcation. Figure 7 illustrates the impact of varying the parameter excitation on the amplitude concerning the Winkler coefficient k_w. Notably, as the parameter excitation declines in the amplitude of the Winkler coefficient and damps at some point (0.1–0.15). Nevertheless, amplitude 1 shows a growing trend while the parametric excitation keeps increasing. Moreover, it is worth noting that the smallest amplitudes occur at a parametric excitation level of $k_w = 1.5$. In Figure 8, the amplitude for a system under parametric excitation depends on both the force amplitude k and the nondimensional damping coefficient c_d. Lower damping generally leads to larger amplitudes near resonance. In contrast, higher damping suppresses oscillations and keeps the amplitude relatively low. Critical damping minimizes the amplitude of the system's response. In Figure 9, the effect of changing the parametric excitation on the amplitude is demonstrated concerning the uniaxial magnetic field H_x. Initially, as the parameter excitation declines in the amplitude and damps at some point (0.1–0.15). However, the amplitude exhibits a rising trend as the parametric excitation increases. It is noteworthy that the smallest amplitudes are observed at a parametric excitation level of $H_x = 0.5$. The relationship between the parametric excitation and amplitude for various temperature levels is depicted in Figure 10. It was found that there was a gradual decrease in temperature starting at around 1.0 and damping at some point (0.1–0.15). On the other hand, the amplitude shows a rising trend while the parametric excitation keeps increasing. Notably that the smallest amplitudes

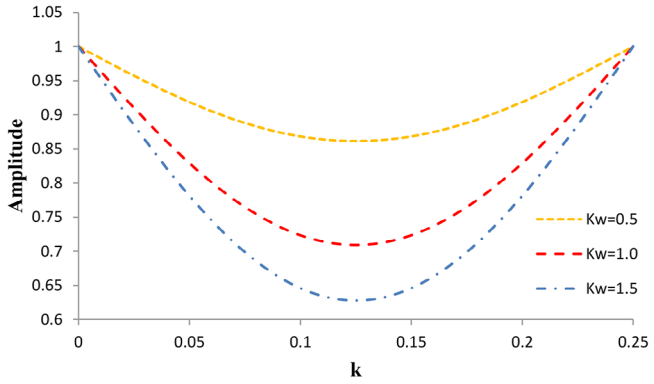

FIGURE 7 The effect of parametric excitation (k) on the amplitude of parametric excitation (a) for different values of Winkler coefficient (k_w).

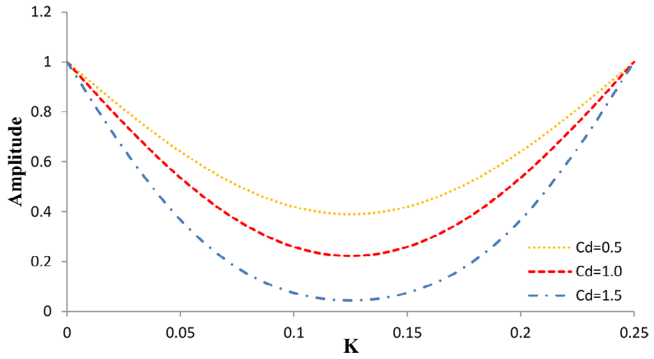

FIGURE 8 The effect of parametric excitation (k) on the amplitude of parametric excitation (a) for different values of damping coefficient (c_d).

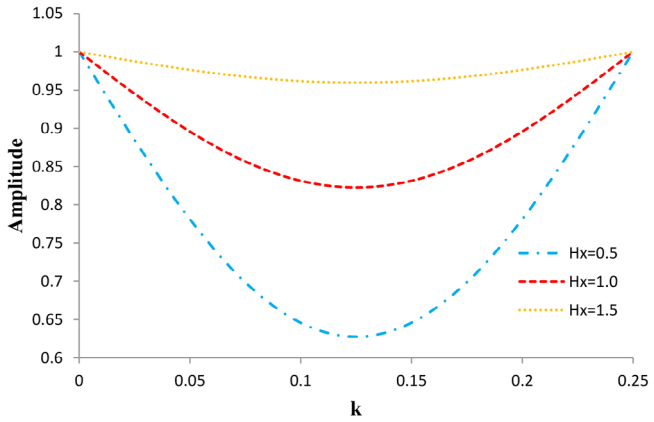

FIGURE 9 The effect of parametric excitation (k) on the amplitude of parametric excitation (a) for different values of uniaxial magnetic field (H_x).

are observed at a parametric excitation level of $T = 300$. In Figure 11, the relationship between parametric excitation and amplitude is illustrated across various values of the nondimensional nonlocal parameter γ. A resonant behavior is evident as the γ value gradually decreases, starting from approximately 1.0 and tapering off between 0.1 and 0.15. This resonance is attributed to the combined effects of parametric excitation and amplitude on the system. Figures 12 and 13 show 3D surface curves for the amplitude "a" to study the nonlinear vibration and parametric excitation of magneto-thermo elastic embed-

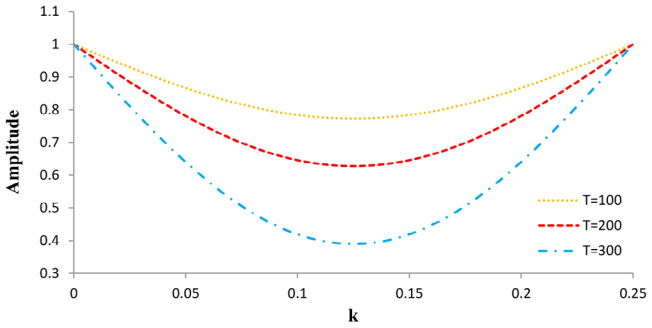

FIGURE 10 The effect of parametric excitation (k) on the amplitude of parametric excitation (a) for different values of temperature (T).

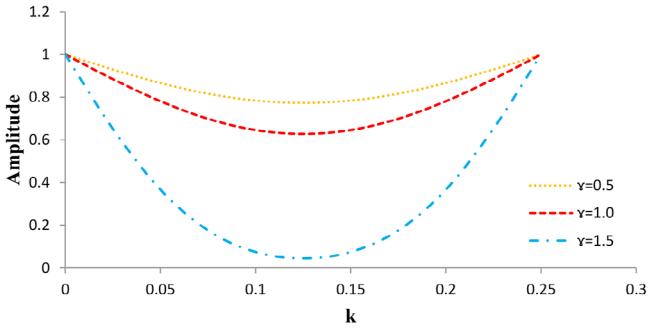

FIGURE 11 The effect of parametric excitation (k) on the amplitude of parametric excitation (a) for different values of nondimensional nonlocal parameter (γ).

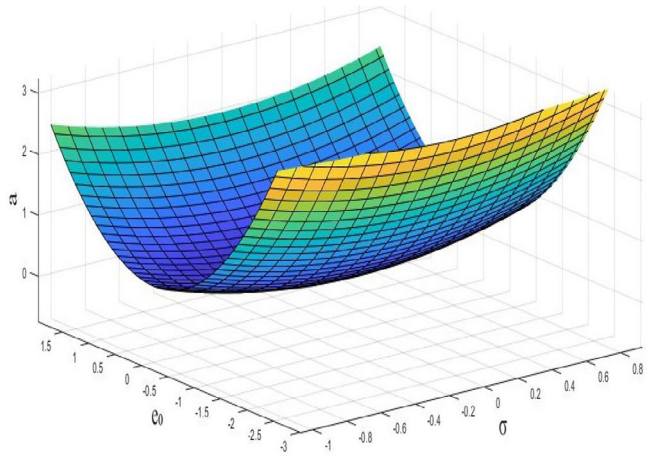

FIGURE 12 The effect of amplitude of parametric excitation in the context of nonlinear frequency and nonlocal parameter for the values of $k = 0.2$.

ded nanobeam. These figures are significant to study the dependence of these physical fields on the horizontal component of distance. Whenever nonlinear frequency and nonlocal parameters increase, the amplitudes oscillate for different values of k ($k = 0.2$ and $k = 0.4$). Figures 14–16 reveal a consistent positive correlation between the variables x and e_0 with the dependent variables σ_{xx}, H_x, and σ. As x and e_0 increase, all three dependent variables tend to rise. Specifically, σ_{xx} and H_x show a moderate increase, while σ displays a broader range of variation, indicating its greater sensitivity to changes in x and e_0.

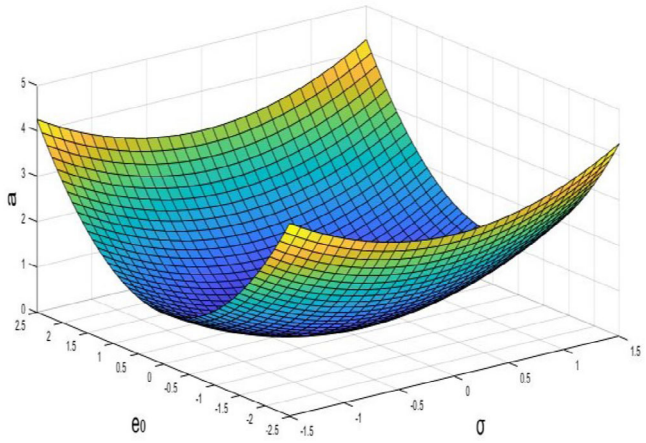

FIGURE 13 The effect of amplitude of parametric excitation in the context of nonlinear frequency and nonlocal parameter for the value of $k = 0.4$.

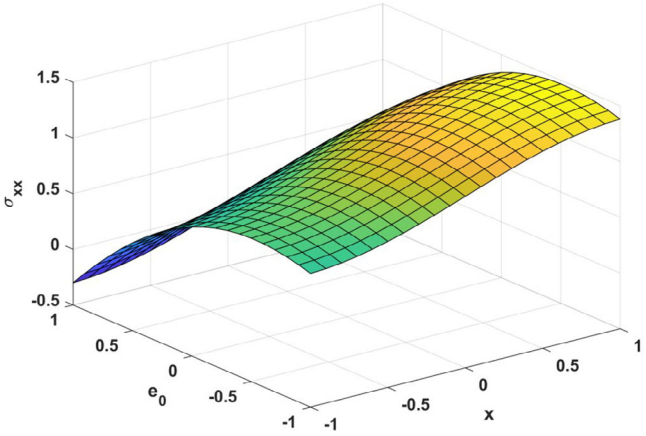

FIGURE 14 The effect of normal-stress (σ_{xx}) with the distance (x) and nonlocal parameter (e_0).

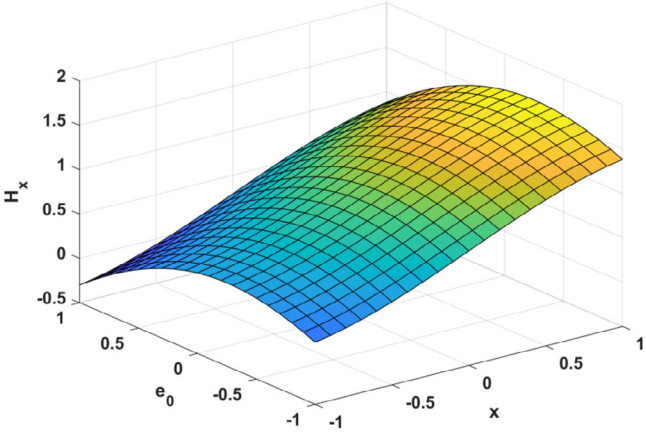

FIGURE 15 The effect of uniaxial magnetic field (H_x) with the distance (x) and nonlocal parameter (e_0).

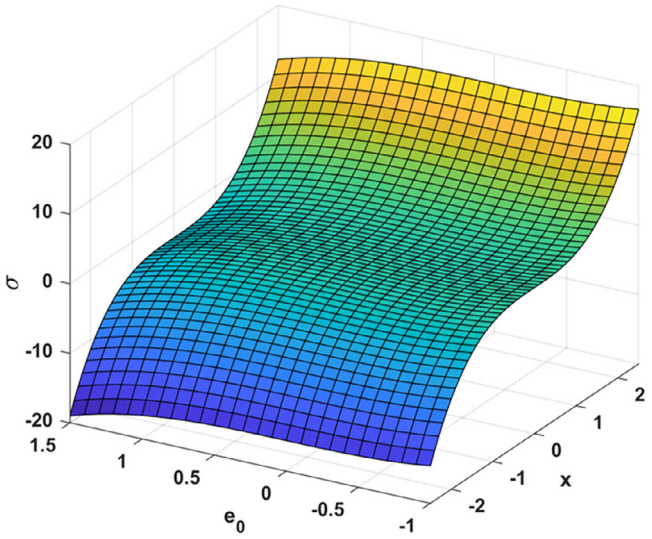

FIGURE 16 The effect of nonlinear frequency (σ) with the distance (x) and nonlocal parameter (e_0).

5 | CONCLUSION

This research aims to examine the dynamic parametric excitation and nonlinear vibration behavior of Euler-Bernoulli nanobeams under thermo-magneto-mechanical loading. Initially, a concise model of the Euler–Bernoulli nanobeam is developed and subjected to parametric external excitation. Utilizing the nonlocal continuum theory and nonlinear von Karman beam theory, the governing nonlinear differential equation of motion is derived. The partial differential equation is then converted into an ordinary differential equation using the HPT. Next, the Euler-Bernoulli nanobeam modulation equation is found. Special attention is given to the influence of parametric excitation, and bifurcation points are scrutinized to delineate instability regions. Notably, it is observed that the damping coefficient, along with parametric excitation, significantly affects the system stability and frequency responsiveness. Thermo-magneto-mechanical loads are found to induce either growth or decay in the amplitude. The following is a list of the study's other main results:

1. The damping coefficient significantly influences system stability, while factors such as the nonlocal parameter and Winkler coefficient are less important.
2. The influence of parametric excitation induced by an external axial force on system stability is substantial.
3. Amplitude response is observed to vary as a function of the excitation frequency. For initial amplitudes of significant magnitude, the response decays until reaching a steady-state solution.
4. An increase in force amplitude leads to a notable separation between stable and unstable curves, creating a gap between them.
5. The numerical results serve as reference points for conducting further analyses of nanobeams, which serve as fundamental components in nanoelectromechanical systems.

ACKNOWLEDGMENTS
The authors have nothing to report.

CONFLICT OF INTEREST STATEMENT
The authors declare no conflicts of interest.

ORCID
Rajendran Selvamani https://orcid.org/0000-0001-5166-5449
Prabhakaran Thangamuni https://orcid.org/0009-0007-7897-0356
Murat Yaylacı https://orcid.org/0000-0003-0407-1685
Mehmet Emin Özdemir https://orcid.org/0000-0001-7983-7265
Ecren Uzun Yaylacı https://orcid.org/0000-0002-2558-2487

REFERENCES

[1] Eda, G., Fanchini, G., Chhowalla, M.: Large-area ultrathin films of reduced grapheme oxide as a transparent and flexible electronic material. Nat. Nanotechnol. 3(5), 270–274 (2008). https://doi.org/10.1038/nnano.2008.83

[2] Li, D., Müller, M.B., Gilje, S., Kaner, R.B., Wallace, G.G.: Processable aqueous dispersions of graphene nanosheets. Nat. Nanotechnol. 3(2), 101–105 (2008). https://doi.org/10.1038/nnano.2007.451

[3] Huang, Y., Zheng, H., Chen, X., Feng, M.: Instability analysis of quasicrystal nano-switch with thermal effect and surface distributed forces. Z Angew Math Mech. 103(10), e202200268 (2023). https://doi.org/10.1002/zamm.202200268

[4] Feng, X., Zhang, L., Li, Y., Gao, Y.: Electromechanical coupling characteristics of multilayered piezoelectric quasicrystal plates in an elastic medium. Z Angew Math Mech. e202300464 (2024). https://doi.org/10.1002/zamm.202300464

[5] Potekin, R., Kim, S., McFarland, D.M., Bergman, L.A., Cho, H., Vakakis, A.F.: A micromechanical mass sensing method based on amplitude tracking within an ultra-wide broadband resonance. Nonlinear Dynam. 92(2), 287–304 (2018). https://doi.org/10.1007/s11071-018-4055-y

[6] Mahmoud, M.A.: Validity and accuracy of resonance shift prediction formulas for microcantilevers: A review and comparative study. Crit. Rev. Solid State Mater. Sci. 41(5), 386–429 (2016). https://doi.org/10.1080/10408436.2016.1142858

[7] Ji, Y., Choe, M., Cho, B., Song, S., Yoon, J., Ko, H.C., Lee, T.: Organic nonvolatile memory devices with charge trapping multilayer graphene film. Nanotechnology 23(10), 105202 (2012). https://doi.org/10.1088/0957-4484/23/10/105202

[8] Arash, B., Wang, Q.: Detection of gas atoms with carbon nanotubes. Sci. Rep. 3, 1782 (2013). https://doi.org/10.1038/srep01782

[9] Bunch, J.S., Van Der Zande, A.M., Verbridge, S.S., Frank, I.W., Tanenbaum, D.M., Parpia, J.M., McEuen, P.L.: Electromechanical resonators from graphene sheets. Science 315(5811), 490–493 (2007). https://doi.org/10.1126/science.1136836

[10] Kuilla, T., Bhadra, S., Yao, D., Kim, N.H., Bose, S., Lee, J.H.: Recent advances in graphene based polymer composites. Prog. Polym. Sci. 35(11), 1350–1375 (2010). https://doi.org/10.1016/j.progpolymsci.2010.07.005

[11] Eringen, A.C., Edelen, D.G.B.: On nonlocal elasticity. Int. J. Eng. Sci. 10(3), 233–248 (1972). https://doi.org/10.1016/0020-7225(72)90039-0

[12] Eringen, A.C.: Theories of nonlocal plasticity. Int. J. Eng. Sci. 21(7), 741–751 (1983). https://doi.org/10.1016/0020-7225(83)90058-7

[13] Ghadiri, M., Shafiei, N., Akbarshahi, A.: Influence of thermal and surface effects on vibration behavior of nonlocal rotating Timoshenko nanobeam. Appl. Phys. A 122(7), 673 (2016). https://doi.org/10.1007/s00339-016-0196-3

[14] Sudak, L.J.: Column buckling of multiwalled carbon nanotubes using nonlocal continuum mechanics. J. Appl. Phys. 94(11), 7281–7287 (2003). https://doi.org/10.1063/1.1625437

[15] Zhang, Y.Q., Liu, G.R., Wang, J.S.: Small-scale effects on buckling of multiwalled carbon nanotubes under axial compression. Phys. Rev. B 70(20), 205430 (2004). https://doi.org/10.1103/PhysRevB.70.205430

[16] Barretta, R., Feo, L., Luciano, R., de Sciarra, F.M.: Variational formulations for functionally graded nonlocal Bernoulli–Euler nanobeams. Compos. Struct. 129, 80–89 (2015). https://doi.org/10.1016/j.compstruct.2015.03.033

[17] Ghadiri, M., Safi, M.: Nonlinear vibration analysis of functionally graded nanobeam using homotopy perturbation method. Adv. Appl. Math. Mech. 9(1), 144–156 (2017). https://doi.org/10.4208/aamm.2015.m899

[18] Ehyaei, J., Akbarshahi, A., Shafiei, N.: Influence of porosity and axial preload on vibration behavior of rotating FG nanobeam. Adv. Nano. Res. 5(2), 141–169 (2017). https://doi.org/10.12989/anr.2017.5.2.141

[19] Ebrahimi, F., Hosseini, S.H.S.: Thermal effects on nonlinear vibration behavior of viscoelastic nanosize plates. J. Therm. Stress 39(5), 606–625 (2016). https://doi.org/10.1080/01495739.2016.1160684

[20] Güçlü, G., Artan, R.: Large elastic deflections of bars based on nonlocal elasticity. Z. Angew. Math. Mech. 100(4), e201900108 (2020). https://doi.org/10.1002/zamm.201900108

[21] Jena, S.K., Pradyumna, S., Chakraverty, S.: Thermal vibration of armchair, chiral, and zigzag types of single walled carbon nanotubes using a nonlocal elasticity theory: An analytical approach. Z Angew Math Mech. 104(4), e202301047 (2024). https://doi.org/10.1002/zamm.202301047

[22] Abouelregal, A.E.: Effect of non-local modified couple stress theory on the responses of axially moving thermoelastic nano-beams. Z. Angew. Math. Mech. 104(4), e202200233 (2024). https://doi.org/10.1002/zamm.202200233

[23] Pisano, A.A., Fuschi, P., Polizzotto, C.: Integral and differential approaches to Eringen's nonlocal elasticity models accounting for boundary effects with applications to beams in bending. Z. Angew. Math. Mech. 101(8), e202000152 (2021). https://doi.org/10.1002/zamm.202000152

[24] Wang, W., Teng, Z.: Analysis of vibration and critical buckling load of porous functionally graded material rectangular nanoplates under thermo-mechanical loading. Z. Angew. Math. Mech. 104(1), e202200073 (2023). https://doi.org/10.1002/zamm.202200073

[25] Simsek, M.: Large amplitude free vibration of nanobeams with various boundary conditions based on the nonlocal elasticity theory. Compos. B Eng. 56, 621–628 (2014). https://doi.org/10.1016/j.compositesb.2013.08.082

[26] Simsek, M.: Nonlinear free vibration of a functionally graded nanobeam using nonlocal strain gradient theory and a novel Hamiltonian approach. Int. J. Eng. Sci. 105, 12–27 (2016). https://doi.org/10.1016/j.ijengsci.2016.04.013

[27] Nazemnezhad, R., Hosseini-Hashemi, S.: Nonlocal nonlinear free vibration of functionally graded nanobeams. Compos. Struct. 110, 192–199 (2014). https://doi.org/10.1016/j.compstruct.2013.12.006

[28] Nourbakhsh, H., Mohammadzadeh, R., Rafiee, M., Rafiee, R.: Nonlinear effects on resonance behaviour of beams in micro scale. In Applied Mechanics and Materials, vol. 110–116, pp. 4178–4186. Trans Tech Publications, Ltd. (2011). https://doi.org/10.4028/www.scientific.net/amm.110-116.4178

[29] Oskouie, M.F., Ansari, R., Sadeghi, F.: Nonlinear vibration analysis of fractional viscoelastic Euler—Bernoulli nanobeams based on the surface stress theory. Acta Mech. Solida Sin. 30(4), 416–424 (2017). https://doi.org/10.1016/j.camss.2017.07.003

[30] Ghadiri, M., Rajabpour, A., Akbarshahi, A.: Non-linear forced vibration analysis of nanobeams subjected to moving concentrated load resting on a viscoelastic foundation considering thermal and surface effects. Appl. Math. Model 50, 676–694 (2017). https://doi.org/10.1016/j.apm.2017.06.019
[31] He, J.H.: A coupling method of a homotopy method and a perturbation technique for non-linear problems. Int. J. Non Linear Mech. 35(1), 37–43 (2000). https://doi.org/10.1016/S0020-7462(98)00085-7
[32] He, J.H.: Addendum: New interpretation of homotopy perturbation method. Int. J. Mod. Phys. B 20(18), 2561–2568 (2006). https://doi.org/10.1142/S0217979206034819
[33] Eltaher, M.A., Mahmoud, F.F., Assie, A.E., Meletis, E.: Coupling effects of nonlocal and surface energy on vibration analysis of nanobeams. Appl. Math. Comput. 224, 760–774 (2013). https://doi.org/10.1016/j.amc.2013.09.002
[34] Reddy, J.: Nonlocal theories for bending, buckling and vibration of beams. Int. J. Eng. Science 45(2-8), 288–307 (2007). https://doi.org/10.1016/j.ijengsci.2007.04.004
[35] Aydogdu, M.: A general nonlocal beam theory: Its application to nanobeam bending, buckling and vibration. Physica E Low Dimens. Syst. Nanostruct. 41(9), 1651–1655 (2009). https://doi.org/10.1016/j.physe.2009.05.014
[36] Alevras, P., Theodossiades, S., Rahnejat, H.: Broadband energy harvesting from parametric vibrations of a class of nonlinear Mathieu systems. Appl. Phys. Lett. 110(23), 233901 (2017). https://doi.org/10.1063/1.4984059
[37] Amer, Y.A., El-Sayed, A.T., Kotb, A.A.: Nonlinear vibration and of the duffing oscillator to parametric excitation with time delay feedback. Nonlinear Dynam. 85(4), 2497–2505 (2016). https://doi.org/10.1007/s11071-016-2840-z
[38] Bobryk, R.V., Yurchenko, D.: On enhancement of vibration-based energy harvesting by a random parametric excitation. J. Sound Vib. 366, 407–417 (2016). https://doi.org/10.1016/j.jsv.2015.11.033
[39] Darabi, M., Ganesan, R.: Non-linear vibration and dynamic instability of internally thickness-tapered composite plates under parametric excitation. Compos. Struct. 176, 82–104 (2017). https://doi.org/10.1016/j.compstruct.2017.04.059
[40] Wang, Y.Z.: Nonlinear internal resonance of double-walled nanobeams under parametric excitation by nonlocal continuum theory. Appl. Math. Model 48, 621–634 (2017). https://doi.org/10.1016/j.apm.2017.04.018
[41] Krylov, S., Harari, I., Cohen, Y.: Stabilization of electrostatically actuated microstructures using parametric excitation. J. Micromech. Microeng. 15(6), 1188 (2005). https://doi.org/10.1088/0960-1317/15/6/009
[42] Yan, Q., Ding, H., Chen, L.: Nonlinear dynamics of axially moving viscoelastic Timoshenko beam under parametric and external excitations. Appl. Math. Mech. 36(8), 971–984 (2015). https://doi.org/10.1007/s10483-015-1966-7
[43] Eringen, A.C.: Nonlocal polar elastic continua. Int. J. Eng. Sci. 10(1), 1–16 (1972). https://doi.org/10.1016/0020-7225(72)90070-5
[44] Eringen, A.C.: On differential equations of nonlocal elasticity and solutions of screw dislocation and surface waves. J. Appl. Phys. 54(9), 4703–4710 (1983). https://doi.org/10.1063/1.332803
[45] Reddy, J.N.: An Introduction to Continuum Mechanics. Cambridge University Press (2013)
[46] Reddy, J.N.: Nonlocal nonlinear formulations for bending of classical and shear deformation theories of beams and plates. Int. J. Eng. Sci. 48(11), 1507–1518 (2010). https://doi.org/10.1016/j.ijengsci.2010.09.020
[47] Emam, S.A.: A static and dynamic analysis of the postbuckling of geometrically imperfect composite beams. Compos. Struct. 90(2), 247–253 (2009). https://doi.org/10.1016/j.compstruct.2009.03.020
[48] Emam, S.A., Nayfeh, A.H.: Postbuckling and free vibrations of composite beams. Compos. Struct. 88(4), 636–642 (2009). https://doi.org/10.1016/j.compstruct.2008.06.006
[49] Murmu, T., McCarthy, M.A., Adhikari, S.: In-plane magnetic field affected transverse vibration of embedded single-layer graphene sheets using equivalent nonlocal elasticity approach. Compos. Struct. 96, 57–63 (2013). https://doi.org/10.1016/j.compstruct.2012.09.005
[50] Kitipornchai, S., He, X.Q., Liew, K.M.: Continuum model for the vibration of multilayered graphene sheets. Phys. Rev. B 72(7), 075443 (2005). https://doi.org/10.1103/PhysRevB.72.075443
[51] Nayfeh, A.H., Mook, D.T.: Nonlinear Oscillations. John Wiley & Sons (2008)
[52] Azrar, L., Benamar, R., White, R.G.: Semi-analytical approach to the non-linear dynamic response problem of S–S and C–C beams at large vibration amplitudes part I: General theory and application to the single mode approach to free and forced vibration analysis. J. Sound Vib. 224(2), 183–207 (1999). https://doi.org/10.1006/jsvi.1998.1893
[53] Azrar, L., Benamar, R., White, R.G.: A semi-analytical approach to the non-linear dynamic response problem of beams at large vibration amplitudes, part II: Multimode approach to the steady state forced periodic response. J. Sound Vib. 255(1), 1–41 (2002). https://doi.org/10.1006/jsvi.2000.3595
[54] Stojanović, V., Petković, M.D.: Dynamic stability of vibrations and critical velocity of a complex bogife system moving on a flexibly supported infinity track. J. Sound Vib. 434, 475–501 (2018). https://doi.org/10.1016/j.jsv.2017.07.057
[55] Stojanović, V., Petković, M.D., Deng, J.: Stability of parametric vibrations of an isolated symmetric cross-ply laminated plate. Compos. B Eng. 167, 631–642 (2019). https://doi.org/10.1016/j.compositesb.2019.02.041
[56] Jena, S.K., Chakraverty, S., Mahesh, V., Harursampath, D., Sedighi, H.M.: A novel numerical approach for the stability of nanobeam exposed to hygro-thermo-magnetic environment embedded in elastic foundation. Z. Angew. Math. Mech. 102(5), e202100380 (2022). https://doi.org/10.1002/zamm.202100380
[57] Selvamani, R., Prabhakaran, T., Rubine, L., Jayan, M., Wang, L.: Vibration of nonhomogeneous porous Euler nanobeams using Bernstein polynomials for boundary characteristics. Songklanakarin J. Sci. Technol. 46(2), (2024)
[58] Li, C., Qing, H.: Integral nonlocal stress gradient elasticity of functionally graded porous Timoshenko nanobeam with symmetrical or anti-symmetrical condition. Z. Angew. Math. Mech. 104(1), e202300282 (2023). https://doi.org/10.1002/zamm.202300282

[59] Ebrahimi, F., Kokaba, M., Shaghaghi, G., Selvamani, R.: Dynamic characteristics of hygro-magneto-thermo-electrical nanobeam with non-ideal boundary conditions. Advances in Nano Res. 8(2), 169–182 (2020). https://doi.org/10.12989/anr.2020.8.2.169
[60] Selvamani, R., Loganathan, R., Dimitri, R., Tornabene, F.: Nonlocal state-space strain gradient wave propagation of magneto thermo piezoelectric functionally graded nanobeam. Curved Layer. Struct. 10(1), 20220192 (2023). https://doi.org/10.1515/cls-2022-0192
[61] Selvamani, R., Prabhakaran, T., Ebrahimi, F.: Damping characteristics of nonlocal strain gradient waves in thermoviscoelastic graphene sheets subjected to nonlinear substrate effects. Phys. Mesomech. 27(4), 461–471 (2024). https://doi.org/10.1134/S1029959924040106
[62] Anitha, L., Rajalakshmi, L., Selvamani, R., Ebrahimi, F.: Forced nonlinear vibrations in a smart magneto-viscoelastic multiscale composite nanobeam in a humid thermal environment. Eng. Trans. 71(4), 617–644 (2023). https://doi.org/10.24423/EngTrans.3114.20231121
[63] Selvamani, R., Rexy, J., Ebrahami, F.: Vibration in an electrically affected hygro-magneto-thermo-flexo electric nanobeam embedded in Winkler-Pasternak foundation. Mech. Adv. Compos. Struct. 8(2), 401–414 (2021). https://doi.org/10.22075/MACS.2021.22068.1311
[64] Selvamani, R., Rubine, L., Rexy, J., Ebrahimi, F.: Dispersion analysis of electrically actuated hygro-magneto-thermo-flexo electric nanobeam embedded on silica aerogel foundation. Mater. Phys. Mech. 50(1), 1–19 (2022). https://doi.org/10.18149/MPM.5012022_1

How to cite this article: Selvamani, R., Thangamuni, P., Yaylacı, M., Emin Özdemir, M., Yaylacı, E.U.: Nonlinear vibration and parametric excitation of magneto-thermo elastic embedded nanobeam using homotopy perturbation technique. Z Angew Math Mech. e202400525 (2024). https://doi.org/10.1002/zamm.202400525